Acta Oceanol. Sin., 2015, Vol. 34, No. 1, P. 44–54
DOI: 10.1007/s13131-015-0595-x
http://www.hyxb.org.cn
E-mail: hyxbe@263.net

The numerical investigation of seasonal variation of the cold water mass in the Beibu Gulf and its mechanisms

CHEN Zhenhua[1,2,3], QIAO Fangli[2,3]*, XIA Changshui[2,3], WANG Gang[2,3]

[1] College of Physical and Environmental Oceanography, Ocean University of China, Qingdao 266100, China
[2] The First Institute of Oceanography, State Oceanic Administration, Qingdao 266061, China
[3] Key Laboratory of Marine Science and Numerical Modeling (MASNUM), State Oceanic Administration, Qingdao 266061, China

Received 26 May 2014; accepted 11 August 2014

Abstract

A wave-tide-circulation coupled model based on the Princeton Ocean Model is established to explore the seasonal variation of the cold water mass in the Beibu Gulf and its mechanisms. The results show that the cold water mass starts forming in March, reaches the maximum strength during June and July, and fades away since October. Strong mixing in winter transports the cold water from sea surface to bottom. The cold water mass remains in the bottom layer as the thermocline strengthens during spring, except for the shallow water where the themocline is broken by strong tidal mixing, which gradually separate the cold water mass from its surrounding warm water. Further analysis on the ocean current and stream function confirms that the cold water mass in the Beibu Gulf is locally developed, with an anticlockwise circulation caused by a strong temperature gradient. Sensitivity experiments reveal that the cold water mass is controlled by the sea surface heat flux, while the terrain and tidal mixing also play important roles.

Key words: Beibu Gulf, cold water mass, seasonal variation, wave-tide-circulation coupled model

Citation: Chen Zhenhua, Qiao Fangli, Xia Changshui, Wang Gang. 2015. The numerical investigation of seasonal variation of the cold water mass in the Beibu Gulf and its mechanisms. Acta Oceanologica Sinica, 34(1): 44–54, doi: 10.1007/s13131-015-0595-x

1 Introduction

The Beibu Gulf (BG) is located in the northwest South China Sea (SCS), as a shallow semiclosed gulf with the averaged depth of about 40 m (Fig. 1). It also is listed as one of the four major fishing grounds of China. Cold water mass (CWM) plays an important role in forming the circulation structure and marine ecosystem in the BG. Compared with the Yellow Sea CWM, few studies have been carried out on the Beibu Gulf CWM (BGC). Therefore, there is a great need to investigate the BGC.

The BGC was first reported by the Sino-Vietnam's joint marine survey in May 1960, and also reported in several surveys later on, including those in May 1994 (Zhong, 1995) and in May 2007 (Huang et al., 2009). The BGC appears in the bottom layer off east Bailongwei Island in the northern BG (20°–21°N, 108°–109°E) (Fig. 2), with core temperature below 21°C, 3–4°C lower than the surrounding seawaters. Su (2005) summarized that the BGC might form in April, mature during June and July, and disappear in September. But previous researches on the BGC are largely based on surveys limited to the eastern BG (Huang et al., 2009), except for the two surveys carried out in 1960 and 1962 covering the whole gulf. The patchier survey data might lead to insufficient understanding of the BGC.

The numerical simulation is a useful tool to compensate for limited observations. However, previous numerical studies on the BG seldom addressed the BGC, but focused more on tides and circulation structures. So far, the continuous variation of the BGC and its mechanisms remain unclear. The BG is characterized by strong tidal motion (Fang et al., 1999; Shi et al., 2002), and tidal mixing can influence the cold water mass (Zhao, 1986; Xia et al., 2006). However, previous efforts rarely account for the impact of tidal mixing on the BGC. The terrain plays an important role in formation of the Yellow Sea CWM (Xu et al., 2003), but the influence of the terrain on the BGC remains unclear. Besides, related studies have provided various views that need to be tested, for example, whether the circulation in the BG during summer runs anticlockwise (Manh and Yanagi, 2000; Xia et al., 2001; Wu et al., 2008) or clockwise (Liu and Yu, 1980; Wang, 1998; Sun et al., 2001). The uncertainties might result from diagnostic model without comprehensive physical processes, using different forcing inputs.

In this study, a high-resolution wave-tide-circulation coupled model, including physical processes such as wind, waves, tide, heat flux, evaporation, rainfall, and runoffs, is established to reproduce the monthly variation and horizontal current of the BGC. Three sensitive experiments are designed to examine the impacts of the sea surface heat flux, terrain and tidal mixing on the BGC, respectively.

The rest of this paper is organized as follows: Section 2 gives configuration of this model; in Section 3, we validate the model using field observations; the seasonal variation and three-dimensional structure of the BGC is reproduced in Section 4; in Section 5, sensitive experiments are designed to reveal dynamic mechanisms of the BGC, and then compare with that of the Yellow Sea CWM; and Section 6 is the summary of this work.

2 Numerical model and experiment design

A wave-circulation coupled model (Qiao et al., 2004; Qiao

Foundation item: The National Natural Science Foundation of China under contract No. U1406404; the National Basic Research Program (973 Program) of China under contract No. 2014CB745004.
*Corresponding author, E-mail: qiaofl@fio.org.cn

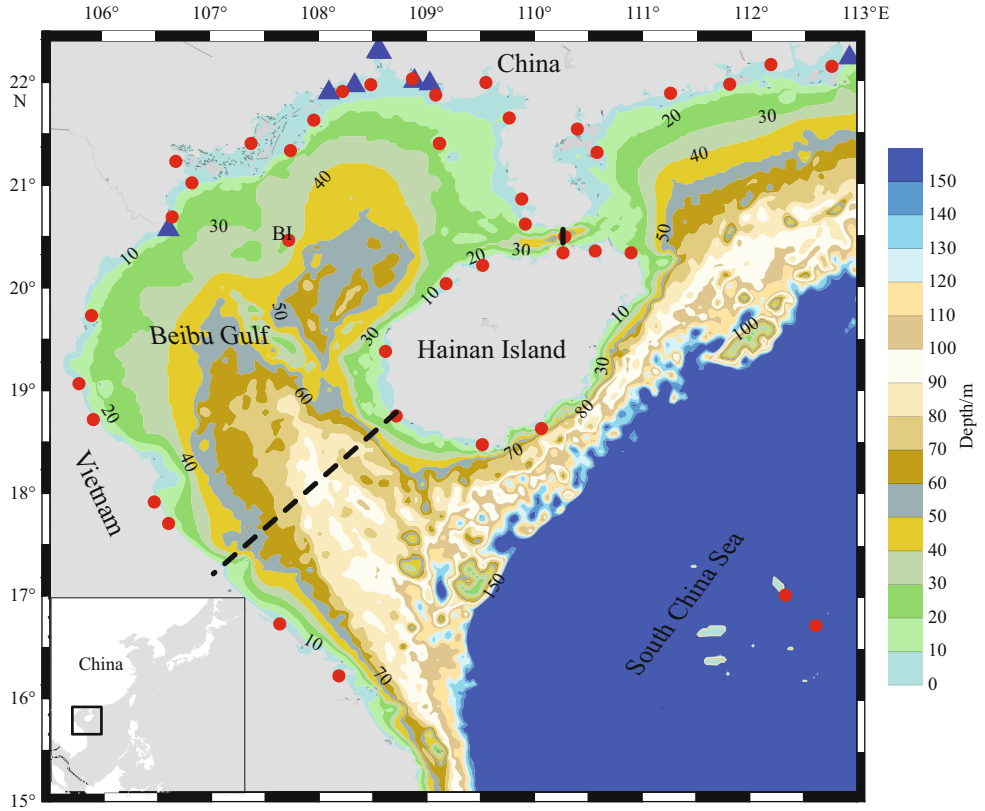

Fig. 1. Map of the study area. The dashed line indicates the boundary of the Beibu Gulf. The red dots indicate tide stations and the blue triangles, runoffs. BI stands for Bailongwei Island.

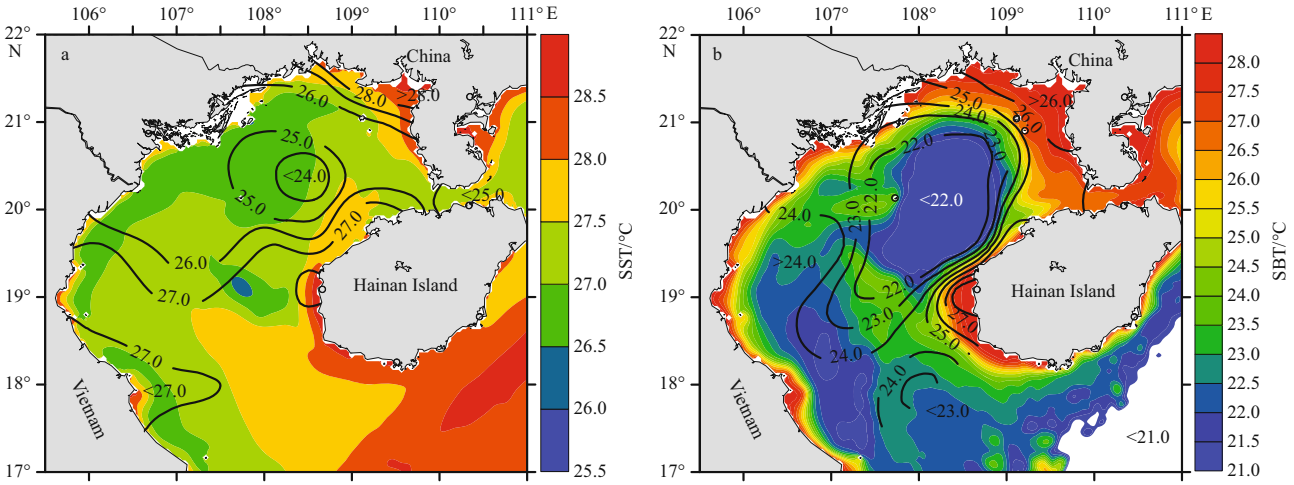

Fig. 2. Color blocks indicate simulated SST (sea surface temperature) (a) and SBT (sea bottom temperature) (b) in May, the black contours are observed SST (a) and SBT (b) in May 1960 from the Sino-Vietnam's joint survey (STCPRC, 1964).

et al., 2006; Qiao et al., 2010) performs well in simulating the thermohaline circulation of the upper layer (Lin et al., 2006; Xia et al., 2006). It will be adopted in this study to explore the BGC. This wave-tide-circulation coupled model is based on the Princeton Ocean Model (POM). Conventional POM uses the level 2.5 Mellor and Yamada (M-Y2.5) turbulence closure scheme (Mellor and Yamada, 1982) to calculate vertical turbulence mixing. Qiao et al. (2004) however introduced a factor of wave-induced vertical viscosity/diffusivity into the vertical mixing scheme. The factor is expressed as a function of wavenumber spectrum:

$$B_{\mathrm{v}} = \alpha \iint_{\vec{k}} E(\vec{k}) \exp(2kz)\,\mathrm{d}\vec{k} \times \frac{\partial}{\partial z}\left[\iint_{\vec{k}} \omega^2 E\left(\vec{k}\right) \exp(2kz)\,\mathrm{d}\vec{k}\right]^{1/2}, \quad (1)$$

where $E(\vec{k})$ represents the wave-number spectrum; ω is the wave angular frequency; $\vec{k}$ is the wavenumber, and z is the vertical coordinate with z=0 on the mean sea surface and positive upward. B_{v} is a factor determining the wave-induced mixing strength, and is added to the coefficient calculated from Mellor-Yamada scheme:

$$K_m = K_{mc} + B_v,$$
$$K_h = K_{hc} + B_v. \quad (2)$$

To calculate B_v, we use the Laboratory of Marine Science and Numerical Modeling (MASNUM) wave model (Yang et al., 2005).

The model domain encompasses the Beibu Gulf, Hainan Island and the Qiongzhou Strait (105.5°–113°E, 15°–22°N) (Fig. 1) to reduce the influence by boundary conditions. The spatial resolution is 2′ by 2′ with 21 sigma levels in the vertical (0, –0.002, –0.004, –0.008, –0.017, –0.033, –0.067, –0.133, –0.200, –0.267, –0.333, –0.400, –0.467, –0.533, –0.600, –0.667, –0.733, –0.800, –0.867, –0.933, –1.000). The topography is based on the ETOPO1 data (Amante and Eakins, 2009), with a minimum depth of 3 m. It is corrected by a sea chart for the regions near the Qiongzhou Strait and Hainan Island. Four tidal constituents, K_1, O_1, M_2, and S_2, are considered in the simulation. The tidal harmonic constants at the open boundary are derived from the Oregon State University tidal model (http://volkov.oce.orst.edu/tides/YS.html), which has a horizontal resolution of (1/30)° in the China seas (Zu et al., 2008).

We use 6 hourly climatological wind data derived from QuikSCAT as the surface forcing. The wind stress is calculated using Large and Pond (1981) and Trenberth et al. (1990). The monthly climatological net heat flux is from a comprehensive ocean-Atmosphere data set (COADS)(Da Silva et al., 1994). The heat flux is applied following Haney (1971):

$$Q = Q_c + \left(\frac{dQ}{dT}\right)_c (T_c^o - T^o), \quad (3)$$

where subscript c represents the data from the COADS; Q_c is the net heat flux; dQ/dT is the partial derivative of the net heat flux relative to sea surface temperature (SST); T_c^o is the climatological monthly mean SST from the COADS; and T^o is model SST.

The climatologically monthly evaporation and precipitation used in the model are also taken from the COADS. The climatologically monthly runoffs of the Red River of Vietnam, and the Zhujiang River, Nanliu River, Dafeng River, Qin River, Fangcheng River and Beilun River of China are considered. The runoff of the Zhujiang River enters the SCS through the YAMEN outlet that is the nearest to the Beibu Gulf. Runoff of the Red River is from Chen et al. (2012) and that of the other rivers are referenced to Gao et al. (2013). The temperature and salinity fields are initialized using Levitus (1982) annual mean temperature and salinity. Open lateral boundary conditions (elevation, velocity, temperature, and salinity) are interpolated from the output of a Pacific model of (1/8)°×(1/8)° resolution (Xia et al., 2004; Xia et al., 2006), which is also a MASNUM wave-tide-circulation coupled model, whose domain is (0°–50°N, 99°–150°E). Flather's (1976) boundary condition is applied to relating a velocity and elevation, and an upwind advection is adopted for the temperature and the salinity.

The model is integrated for 8 years for the equilibrium state, the result for the eighth year, representing a multiyear mean level is analyzed.

Besides the standard modeling (the control run), three sensitivity experiments, NoHeat, NoTide and Topotest are designed (Table 1) and carried out to examine the roles of the surface heat flux forcing, the tidal forcing and the terrain, respectively. In experiment NoHeat, the surface heat flux is removed from the model while other physical processes are kept unchanged; in Experiment NoTide, similarly, the tides are excluded from the model; in experiment Topotest, the central mouth of the south BG remains unchanged, while the other part of this gulf is changed to a flat bottom, with a water depth of 20 m (Fig. 3a), no change is made for the other configurations.

3 Model validation

3.1 *Tide*

At first, the model was run with tidal forcing and homogenous water only, by setting temperature at 20°C and salinity at 35 in the whole model domain. Through a harmonic analysis, we obtain the harmonic constants of the partial tide K_1, O_1, M_2, and S_2, and then compare our simulations with the constants from 42 tidal stations (Fig. 1). For the tidal constituents K_1, O_1, M_2, and S_2, their mean absolute errors of amplitude are 4.7, 5.3, 4.5, and 3.5 cm, respectively, and the phase errors are 5.6°, 6.0°, 10.4°, and 10.7°, respectively. The simulated cotidal and coamplitude lines agree well with previous studies (e.g., Fang et al., 1999; Zhao et al., 2010).

3.2 *Temperature*

Figure 4 shows differences between the simulated and satellite-derived SSTs in February, May, August and November, representing the four seasons. The climatological monthly-mean satellite SST is taken as the reference, which is calculated from daily REMSS (the remote sensing systems) SST product provided by the NASA for 2006–2010, at a spatial resolution of 9 km by 9 km. Compared with the reference SST, minor differences within ±0.6°C can be seen in most areas in each month, indicating that the model surface temperature accords with the observation.

The simulation shows a low-temperature core in May on the bottom of the northern central BGC (107.5°–109.0°E, 19.5°–21.0°N) (Fig. 2b), with a temperature around 22°C, which is about 2–3°C lower than its surrounding seawater. In addition to the temperature, the scope of this CWM is also quite consistent with that observed during the Sino-Vietnam's joint comprehensive marine survey (STCPRC, 1964) (Fig. 2).

3.3 *Salinity*

Figure 5 shows a comparison between the simulated and observed salinity from the Sino-Vietnam's joint survey in 1960 (STCPRC, 1964). The salinity near the coast of Vietnam is quite low but a salinity gradient is large. Tongue-shaped isohalines extend southeastward, probably due to the Red River runoff. Higher salinity water invades from the SCS through the southern BG. The salinity of the BGC ranges from 33.0 to 33.5. The simulated salinity pattern agrees with the observation.

Table 1. Model experiment designs

	Wind	Surface heat flux	Tide	Terrain
Control_run	√	√	√	ETOPO1 plus sea char
NoHeat	√	×	√	ETOPO1 plus sea char
NoTide	√	√	×	ETOPO1 plus sea char
Topotest	√	√	√	flat terrain in 40 m

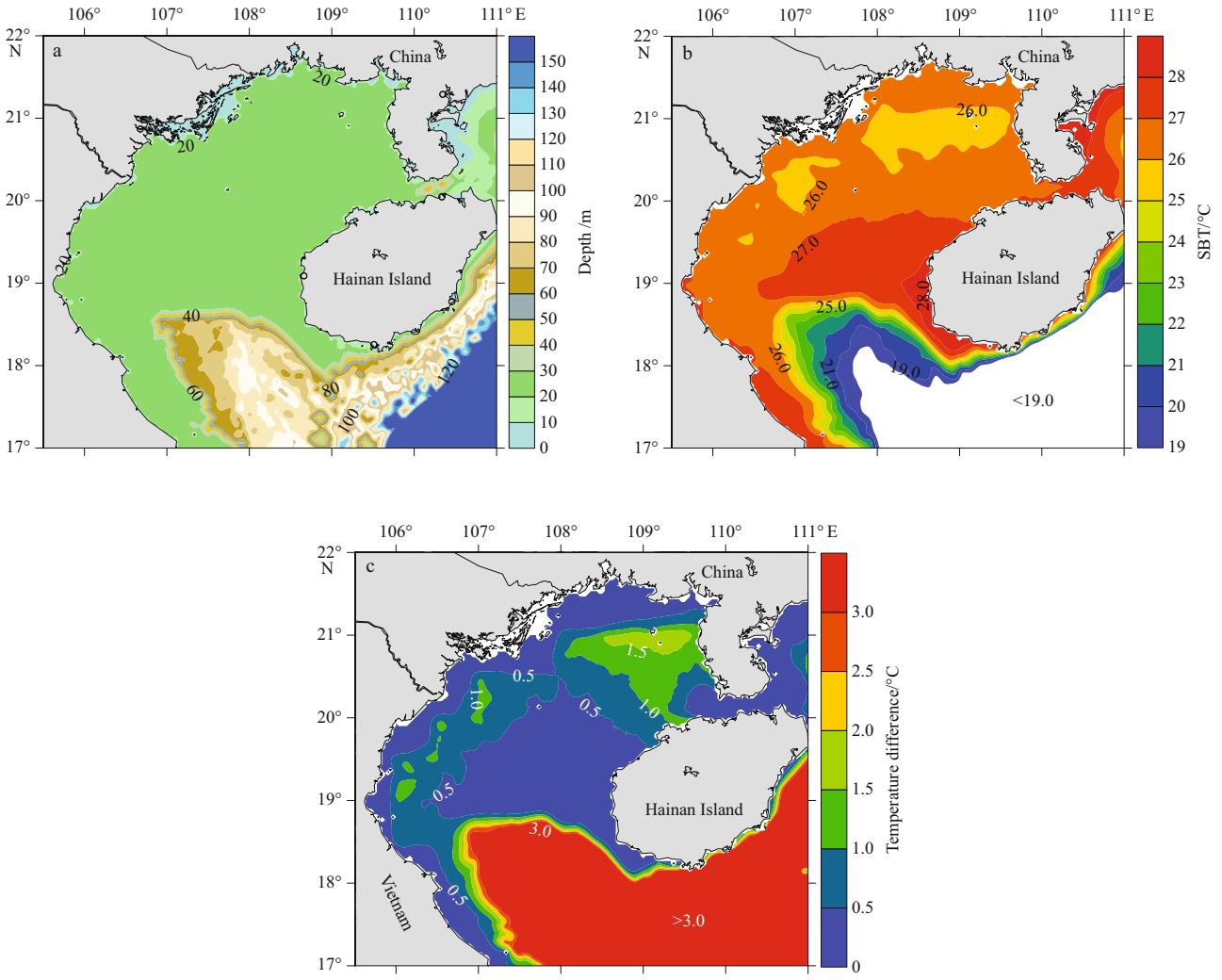

Fig. 3. Results of Experiment Topotest: topographical map (a), SBT (b) and difference between SST and SBT (c) in May.

4 Seasonal variation

The temperature difference (DT) between surface and bottom layers, i.e., SST minus sea bottom temperature (SBT), can reflect seasonal variation of the CWM. Figures 6 and 7 exhibit the DT from March to October, and the vertical temperature distribution along the 20°N cross section.

In winter, due to strong vertical mixing reaching the bottom layer, no BGC is formed. In March, as the surface waters warm up by the solar radiation, the DT increases to 1°C and favors the formation of the BGC. From April to May, the upper layer's stratification intensifies in response to the gradually warming surface, and the DT increases to 4–6°C. The thermocline strengthens rapidly up to 0.48°C/m, and the horizontal temperature gradient also increases. In this context, the BGC is gradually forming, its central temperature increases to at about 21°C. From June to July, the DT reaches its peak at 6–7°C, and the temperature gradient in the thermocline ranges from 0.30 to 0.45°C/m, indicating full development of the CWM. In August, although the SST peaks at 30°C, the DT reduces to 5°C as the SBT warms up. The BGC begins to shrink. In September, the sea surface transfers heat to the atmosphere since the air temperature decreases, the DT drops to 3–4°C because the SST gradually cools, and the BGC continues shrinking. In October, the DT decreases to 3°C in the inner gulf and almost imperceptible in the coastal shallow waters. Eventually, the CWM disappears in November, which is much later than September reported by Su (2005), but is consistent with the report of the Sino-Vietnam's joint survey (STCPRC, 1964). As a whole, the BGC experiences three stages: formation period in spring (from March to May), developing period from June to August, and fading period from September to November.

During the period from April to September (especially May, June and July), the horizontal temperature gradient around the CWM is relatively high (Fig. 6). Figure 8 shows the temperature gradient calculated by Eq. (4), taking the maximum of every vertical layer as the max function. The temperature gradient inside the BGC is small in May (ranging from 0 to 1×10^{-5}°C/m), while that around the BGC can reach 7×10^{-5}–10×10^{-5}°C/m. A temperature front around the BGC even exceeds 10×10^{-5}°C/m to the west of Hainan Island, according to the simulation there by Lü et al. (2008). The temperature front is caused by strong tidal mixing west of Hainan Island (Lü et al., 2008), and then generate anti-clockwise circulation (Fig. 9).

$$G_t = \max\left[\sqrt{\left(\frac{\mathrm{d}T}{\mathrm{d}x}\right)^2 + \left(\frac{\mathrm{d}T}{\mathrm{d}y}\right)^2}\right]. \quad (4)$$

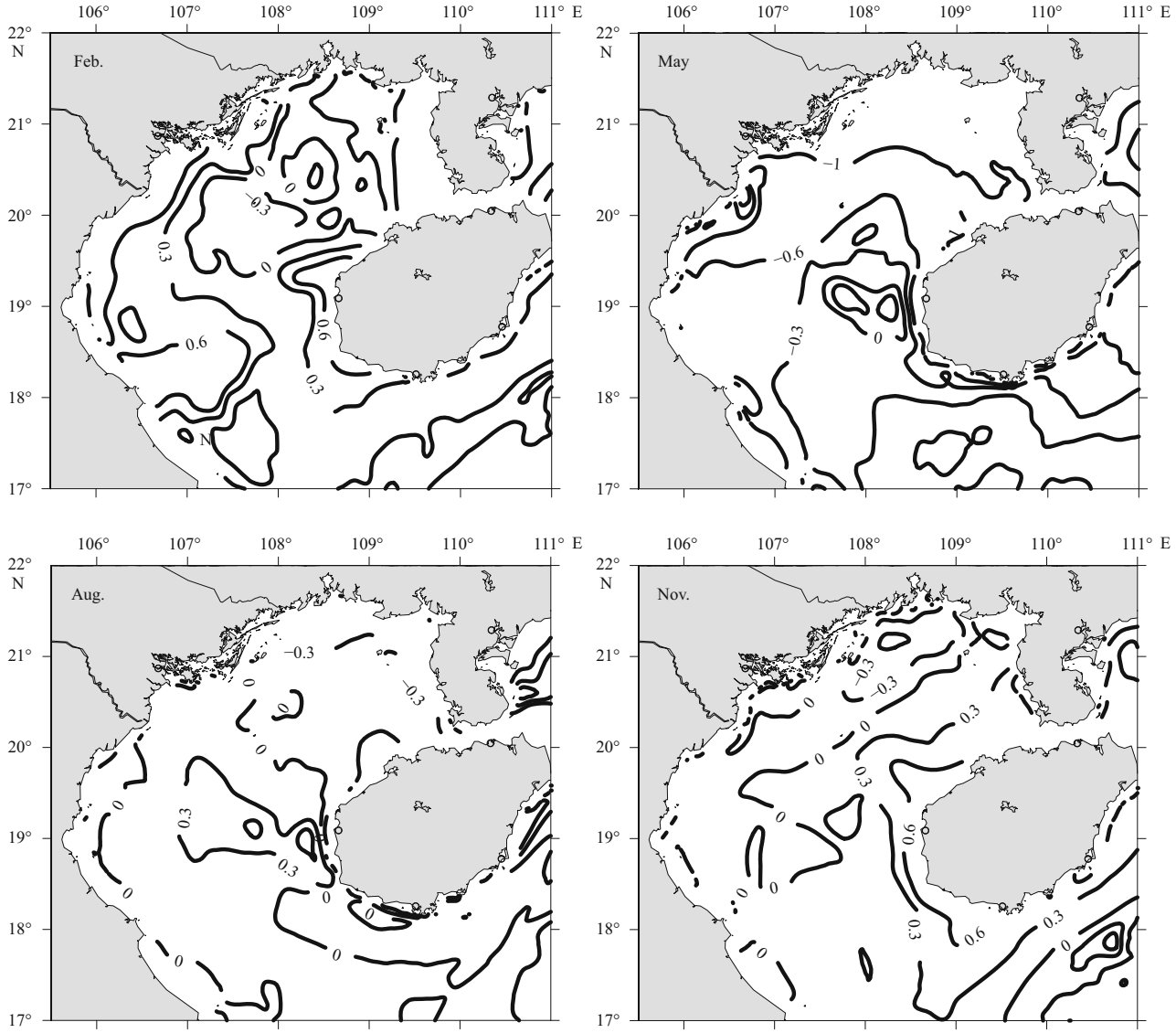

Fig. 4. Difference between simulated SST and REMSS SST in the representative months for the four seasons. Contour interval is 0.3°C.

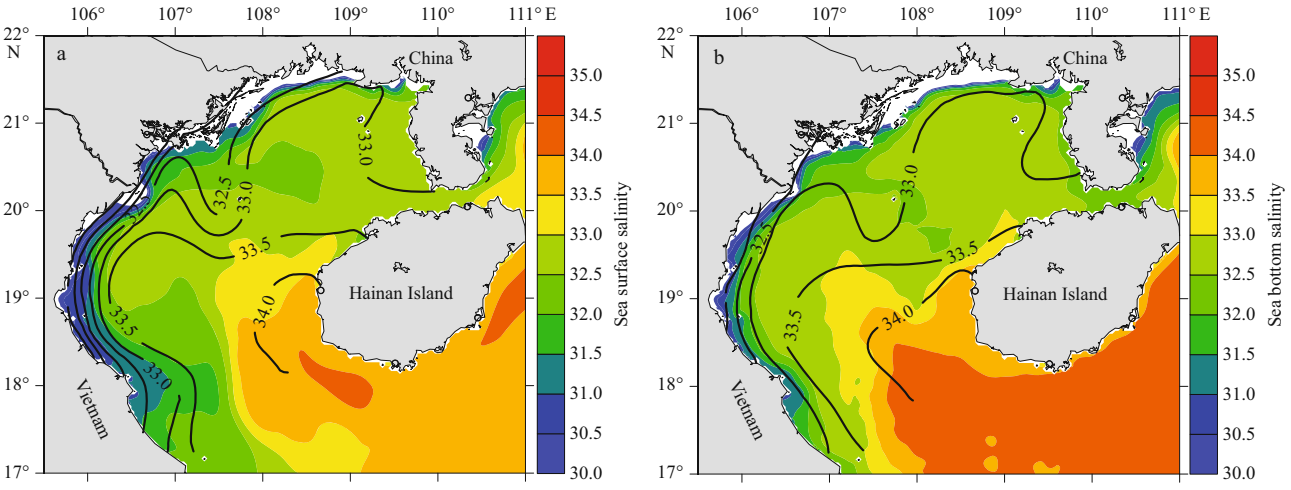

Fig. 5. Color blocks indicate simulated sea surface salinity (a) and sea bottom salinity (b) in April, and the black contours are observed sea surface salinity (a) and sea bottom salinity (b) in April 1960 from the Sino-Vietnam's joint survey (STCPRC, 1964).

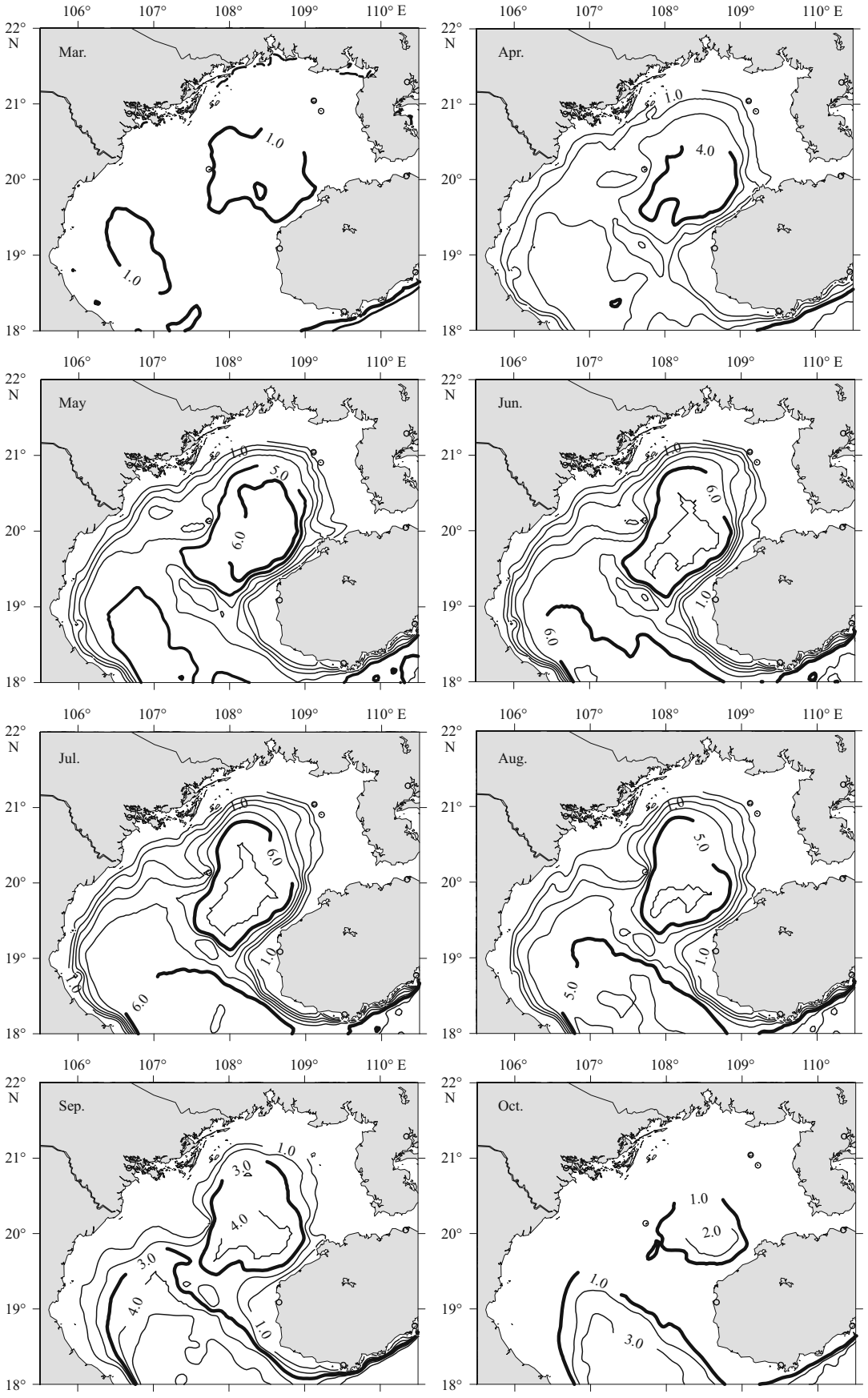

Fig. 6. Difference between SST and SBT from March to October with contour interval of 1°C.

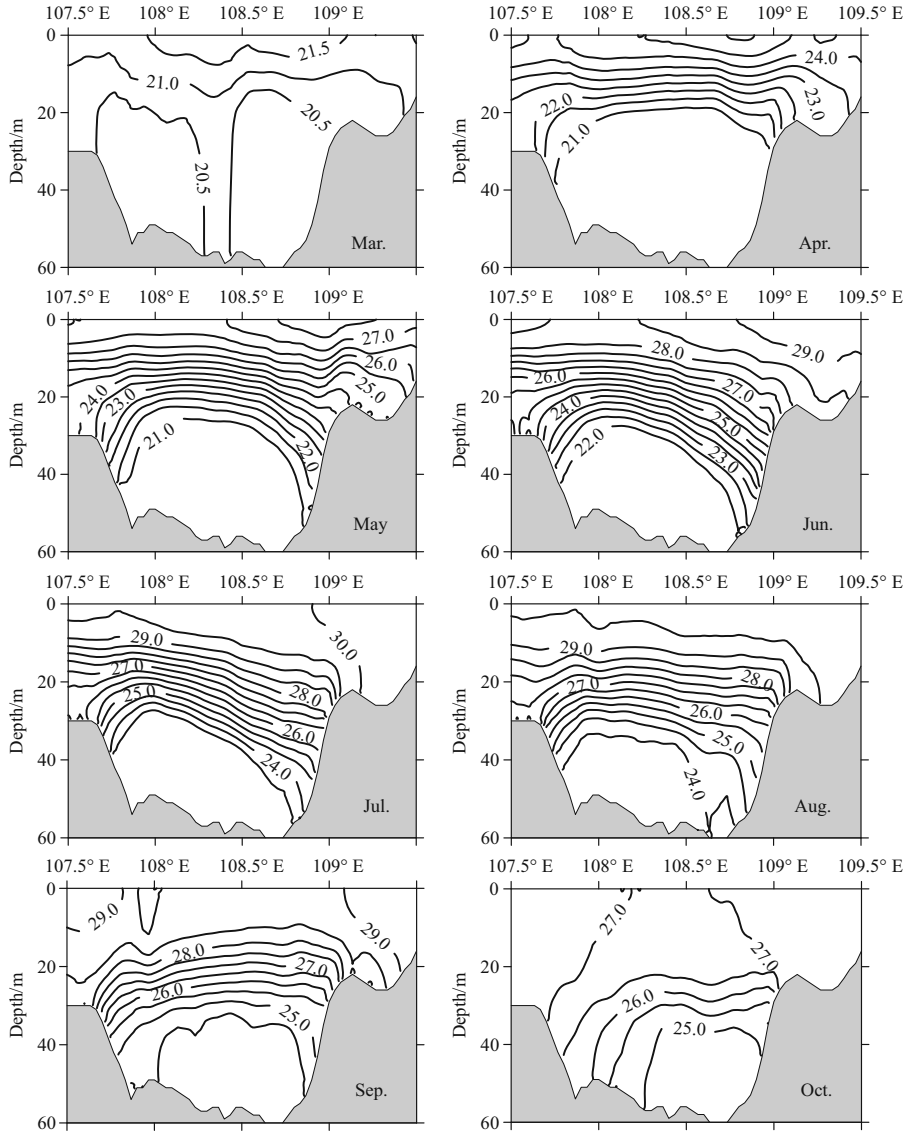

Fig. 7. Vertical distributions of temperature (°C) along 20°N (see Fig. 8 for the transect) from March to October with contour interval of 0.5°C.

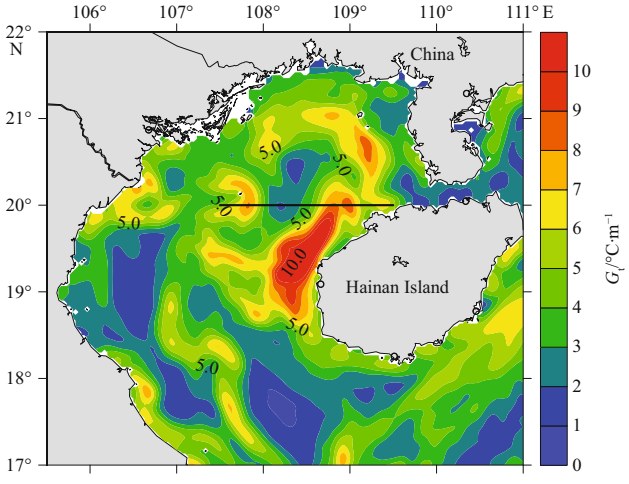

Fig. 8. Temperature gradient in May (in 10^{-5}°C/m). The black line indicates the transect shown in Fig. 7.

5 Dynamic mechanisms

5.1 *Horizontal circulation*

As shown in Fig. 9a, an anticlockwise circulation appears around the BGC in spring, which is caused by the strong temperature gradient. It becomes weaker in summer with its direction unchanged (Fig. 9b), which might be in favor of the maintenance of the CWM. It is contradicted to the result of Wang (1998), which stated that a clockwise circulation around the BGC in summer destroys the BGC.

Another problem is whether the BGC is locally developed. Wang (1998) pointed out that the BGC is a mixture of seawater along the coast and that from the SCS. We calculate the stream function and the vertically averaged flow field in the BG to analyze the water transfer route during the developing period of the BGC in May. Our result, however, indicates that a horizontal flow appears and the stream function of the BGC forms an enclosed circulation. No horizontal water transport through the CWM is found (Fig. 9). The absence of the water exchange between the BGC and its surrounding water mass or open seas suggests that the BGC is probably locally developed.

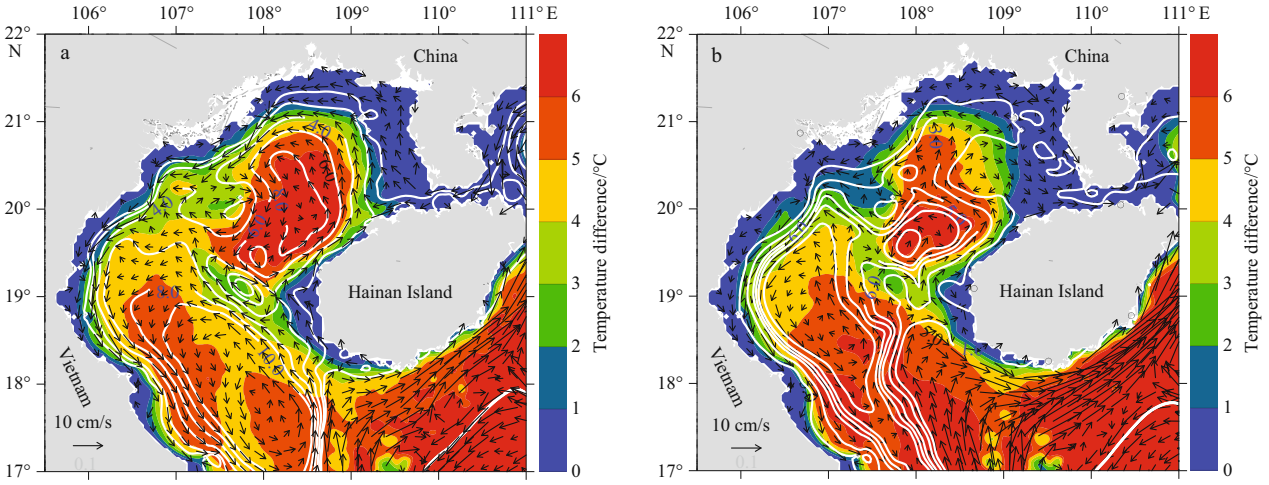

Fig. 9. Difference between SST and SBT in May (a) and August (b). The white contours are a stream function in 10^4 m^3/s, and the black arrows are a vertically averaged velocity.

5.2 *Thermodynamics*

Thermal forcing is of critical importance in formation of the Yellow Sea CWM (Hao et al., 1959; Guan,1963). Zhong (1995) and Wang (1998) also noticed the role of thermal forcing in the BGC, while a model experiment is still needed to test the hypothesis. In our experiment NoHeat (Fig. 10), cold water of about 23°C dominants in the northern BG, and the DT approximates 0–1°C in May. No enclosed cold water patch is found in the area where the BGC occurs in the control run. The experiment result confirms that the BGC is strongly influenced by the surface heat flux forcing.

In winter, the sea surface generally cools down in response to the colder air temperature, which triggers strong mixing that can transport the cold water from surface to bottom. Consequently, a thermocline generates during spring, between the cold water stay in bottom and the warming surface, and then impedes a vertical heat transfer. The CWM therefore is found dominant below the thermocline. When the sea surface heat flux is excluded in the model, the thermocline can no longer take shape since the DT is too small. The CWM, thus, cannot form. It is clear from our experiment that the surface heat flux is an essential factor for the formation of the thermocline that governs the thermodynamics of the BGC.

5.3 *Topographical factor*

In addition to the common terrain of shallow coast and deeper inner gulf, one unique terrain is a bowl-shaped depression on the bottom of the central-northern Beibu Gulf, which can house the cold water there. As wind, wave and tide jointly induce a mixing along the slope of depression, the temperature of shallow water is higher than that of deepwater, so the isothermals curve downwards (Fig. 7) and the temperature front generates (Fig. 8). The consequent anticlockwise frontal circulation (Fig. 9) helps to maintain the BGC.

In the experiment Topotest, the sea temperature changes dramatically. The horizontal and vertical temperatures are becoming more homogeneous. Only in the northeastern gulf, a weak enclosed CWM appears in May in the bottom layer (Figs 3b and c). There is 1°C temperature difference between the BGC and its surrounding, as well between the SST and the SBT. It is because that the bowl-shaped depression is set to flat bottom and the cold water is hard to remain there. Without the slope effect, neither temperature front nor frontal circulation is forming, which enhances the seawater exchange between the gulf and that outside the BG. With stronger mixing, the horizontal and vertical temperatures are becoming more homogeneous. Such small difference might be caused by the solar radiation

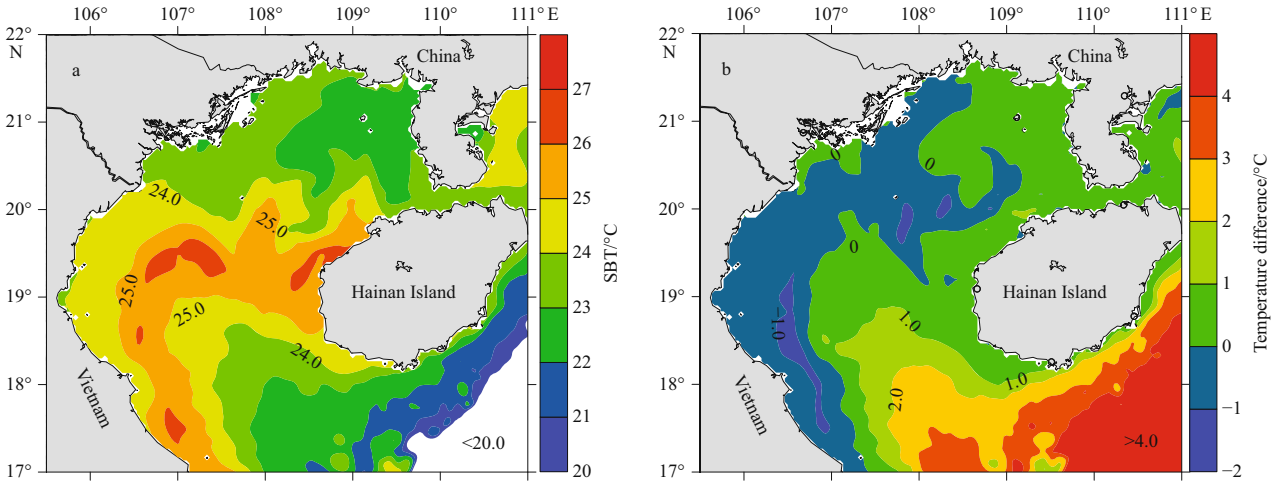

Fig. 10. Simulated SBT (a) and difference between SST and SBT (b) without surface heat flux in May.

and the weak mixing in this region, instead of by the terrain. This weak CWM is very different from that in the control run, both in terms of coverage and temperature, implying that the topography is important for the formation of the BGC.

5.4 *Tidal influence*

Tidal mixing can significantly affect the formation and structure of the CWM in the Yellow Sea (Zhao, 1986; Qiao et al., 2006). As a gulf is characterized by a strong tidal motion, the tidal velocity in the BG was observed to be up to 1.5 m/s near southwest Hainan Island (Sun et al., 2009). In the control experiment, the SBT in May is about 22°C (Fig. 2b), the DT is 5–6°C, and the BGC has distinct profile (Fig. 6). In NoTide experiment, the SBT in May lowers to approximately 19°C, the DT reaches 7–8°C, but the BGC has indistinct profile (Figs 11a and b). The most obvious change is that, in the control run (Fig. 7), isotherms curve downward from the shallow margin of the CWM, exhibiting a table-shape. It is probably due to strong vertical mixing caused by the dissipation of the strong tide on the bottom. In Experiment NoTide, the isotherms distribute in the horizontal direction, no front is formed in the stratified water that lacks tidal mixing (Fig. 11c).

In addition, Experiment NoTide shows that the circulation surrounding the CWM changes from anticlockwise to clockwise in summer (Fig. 11d). The change in the circulation structure is mainly caused by anti-clockwise tidal residual currents (Zu, 2005; Zhao et al., 2010), and by the anticlockwise density circulation formed on the strong temperature front under strong tidal mixing around the BGC (Figs 6 and 7). When the influence of tides is excluded, the circulation becomes clockwise driven by the southwesterly wind in summer. The findings show that tides can dramatically influence the BGC and the circulation in the gulf.

To quantify the influences of the heat flux, terrain and tide on the BGC, we take the mean DT in the areas with the DT exceeding 5°C in May (Fig. 6) as a proxy to indicate the strength of the BGC. In these areas, the mean DT reaches 5.96, 7.00, 0.50 and –0.06°C in the experiments of the control run, NoTide, Topotest and NoHeat, respectively, suggesting that the surface heat flux is a control factor to the BGC, while the tide and terrain also play an important role.

5.5 *Comparison with Yellow Sea cold water mass*

In this part, we give a brief comparison between the BGC and the Yellow Sea CWM. The two CWMs are both located in a semienclosed gulf with distinct seasons, strong tidal motion, and concave slope on bottom. In this context, the two CWMs evolve from similar mechanisms as follows.

They are similar in temperature and circulation structure. In spring and summer, the two closed CWMs occur below the

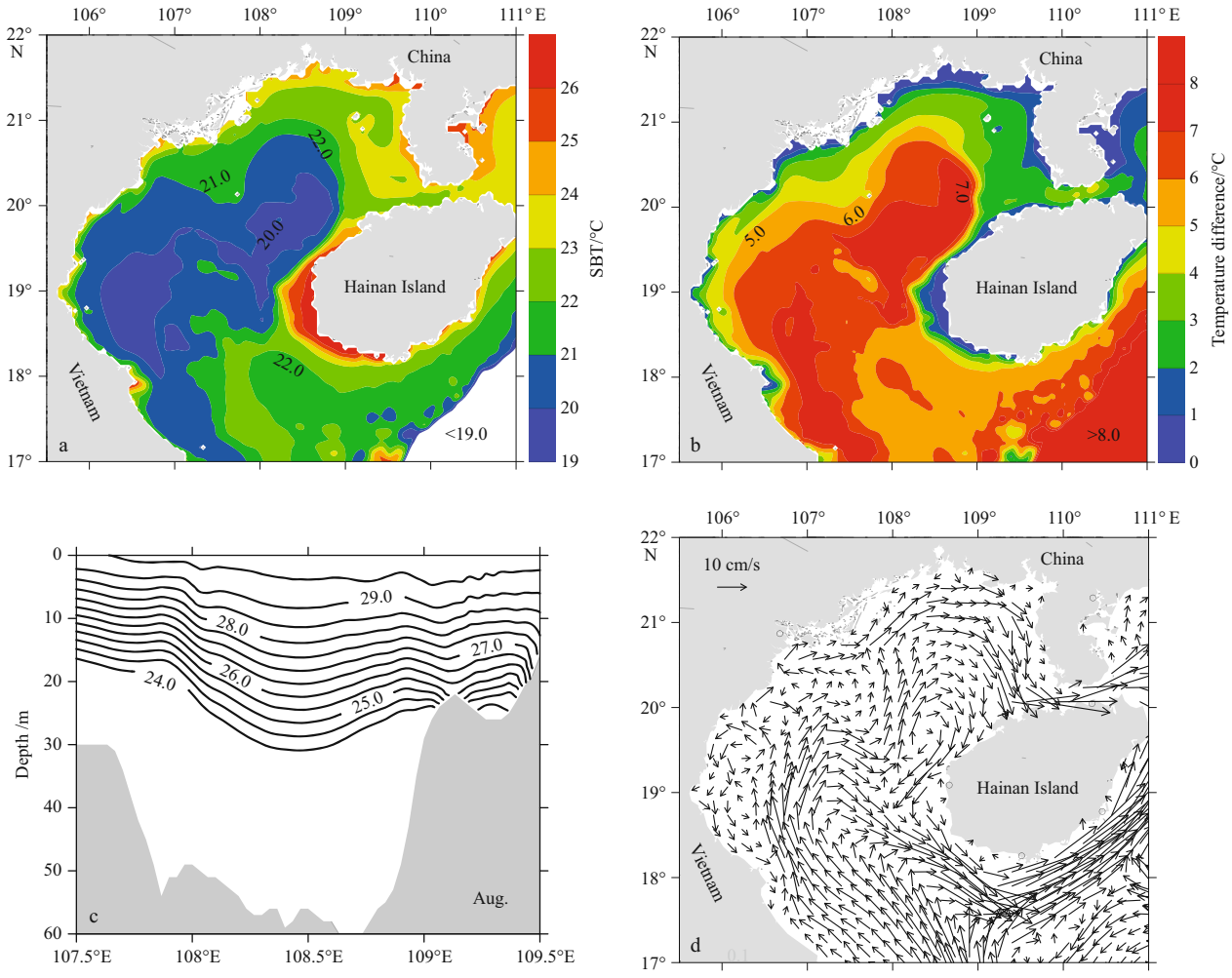

Fig. 11. Results of Experiment NoTide. SBT (a) and difference between SST and SBT (b) in May, vertical distributions of sea temperature (°C) along 20°N (c), and vertically averaged velocity (d) in August.

thermocline, with anticlockwise circulations driven by the strong temperature gradient (Xia et al., 2006).

They are locally developed (Hao et al., 1959; Guan, 1963). The cold water derived from the sea surface during winter houses in the concave. In spring, the cold water remains on the stable deep bottom as seasonal thermocline forms, but the shallow water on the slope warms up because the strong tidal mixing breaks the thermocline, which gradually separates the cold water mass from the surrounding warmer water.

They also have similar life cycle, i.e., forming in spring, developing in summer, and fading in autumn. The cycle is synchronized with the seasonal variation in a surface sea-air heat flux, implying that the heat flux is a controlling factor to the two CWMs.

Meanwhile, some differences exist between the two CWMs, probably due to different water depths and latitude locations. The Yellow Sea is located in a temperate climate zone, and the Beibu Gulf is located in a subtropical climate zone, so the average atmospheric temperature over the Yellow Sea is lower than that over the Beibu Gulf. Besides, the average depth (80 m) of the CWM in the Huanfhai Sea is deeper than that of the Beibu Gulf. As a consequence, the Yellow Sea CWM is more intense and its SBT remains below 8°C throughout the year. In the shallow Beibu Gulf, the SBT of the CWM generally increases from 21 to 25°C during May–October in response to the larger net heat flux in late summer (Fig. 7).

6 Conclusions

Overall, with the inclusion of the integrated physical processes, this model reproduced the thermohaline structure of the Beibu Gulf. Our result is quite consisted with satellite and in situ observation in the Beibu Gulf, demonstrating a convincing simulation.

From the model, the Beibu Gulf cold water mass starts to form in March, reaches the maximum strength during June and July, and has faded away since October. It is likely because that strong mixing during winter transports the cold water from sea surface to bottom layer. In spring, the thermocline generally strengthens and keeps the cold water on the deep concaved bottom. But the thermocline is broken by strong tidal mixing in the shallow water and the water warms up gradually. An isolated cold water mass differed from the surrounding warmer water is then formed. It seems that the effects of the surface heat flux on the cold water mass are superimposed on the effects of terrain and tidal mixing.

Further analysis on the flow filed and the stream function confirms that the BGC is locally developed, with an anticlockwise circulation induced by the strong temperature gradient. Sensitivity experiments reveal that the sea surface heat flux is a controlling factor to the cold water mass, while terrain and tidal mixing also play important roles.

Acknowledgements

The authors would like to thank Yu Zuojun and two anonymous reviewers for their valuable comments and suggestions on the manuscript.

References

Amante C, Eakins B W. 2009. ETOPO1 1 arc-minute global relief model: procedures, data sources and analysis. NOAA Technical Memorandum NESDIS NGDC-24. National Geophysical Data Center, NOAA. doi: 10.7289/V5C8276M

Chen Changsheng, Lai Zhigang, Robert C, et al. 2012. Current separation and upwelling over the southeast shelf of Vietnam in the South China Sea. Journal of Geophysical Research: Oceans (1978–2012), 117(C3), doi: 10.1029/2011JC007150

Da Silva A, Young C C, Levitus S. 1994. Atlas of surface marine data 1994. In: NOAA Atlas NESDIS 6. US Department of Commerce. USA: Silver Spring, 74

Fang Guohong, Kwok Y K, Yu Kejun, et al. 1999. Numerical simulation of principal tidal constituents in the South China Sea, Gulf of Tonkin and Gulf of Thailand. Continental Shelf Research, 19(7): 845–869

Flather R A. 1976. A tidal model of the northwest European continental shelf. Memories Societe Royale Sciences Liege, 6(10): 141–164

Gao Jingsong, Xue Huijie, Chai Fei, et al. 2013. Modeling the circulation in the Gulf of Tonkin, South China Sea. Ocean Dynamics, 63(8): 979–993

Guan Bingxian. 1963. A preliminary study of the temperature variations and the characteristics of the circulation of the Cold Water Mass of the Yellow Sea. Oceanologia et Limnologia Sinica (in Chinese), 5(4): 255–283

Haney R L. 1971. Surface thermal boundary condition for ocean circulation models. Journal of Physical Oceanography, 1(4): 241–248

Hao Chongben, Wang Yuanxiang, Lei Zhongyou, et al. 1959. A preliminary study of the formation of Yellow Sea Cold Mass and its properties. Oceanologia et Limnologia Sinica (in Chinese), 2(1): 11–15

Huang Zhida, Hu Jianyu, Sun Zhenyu, et al. 2009. Distributions of temperature, salinity and density in the eastern Beibu Gulf in spring 2007. In: Li Yan, Hu Jianyu, eds. The Essay Collection of the Researches on the Ocean Science in the Gulf of Tonkin PT II (in Chinese). Beijing: China Ocean Press, 92–99

Large W G, Pond S. 1981. Open ocean momentum flux measurements in moderate to strong winds. Journal of Physical Oceanography, 11(3): 324–336

Levitus S. 1982. Climatological Atlas of the World Ocean, NOAA Professional Paper 13, plus 17 microfiche. Washington, DC: US Government Printing Office, 173

Lin Xiaopei, Xie Shangping, Chen Xinping, et al. 2006. A well-mixed warm water column in the central Bohai Sea in summer: effects of tidal and surface wave mixing. Journal of Geophysical Research, 111: C1107, doi: 10.1029/2006JC003 504

Liu Fengshu, Yu Tienchang. 1980. Preliminary study on the oceanic circulation in Beibu Bay. Transaction of Oceanology and Limnology (in Chinese), (1): 9–15

Lü Xinggan, Qiao Fangli, Wang Guanshuo, et al. 2008. Upwelling off the west coast of Hainan Island in summer: its detection and mechanisms. Geophysical Research Letters, 35(2): L02604

Manh D V, Yanagi T. 2000. A study on residual flow in the Gulf of Tongking. Journal of Oceanography, 56(1): 59–68

Mellor G L, Yamada T. 1982. Development of a turbulence closure model for geophysical fluid problems. Reviews of Geophysics and Space Physics, 20(4): 851–875

Qiao Fangli, Ma Jian, Xia Changshui, et al. 2006. Influences of the surface wave-induced mixing and tidal mixing on the vertical temperature structure of the Yellow and East China Seas in summer. Progress in Natural Science, 16(7): 739–746

Qiao Fangli, Yuan Yeli, Ezer T, et al. 2010. A three-dimensional surface wave-ocean circulation coupled model and its initial testing. Ocean Dynamics, 60(5): 1339–1355

Qiao Fangli, Yuan Yeli, Yang Yongzeng, et al. 2004. Wave-induced mixing in the upper ocean: Distribution and application to a global ocean circulation model. Geophysical Research Letters, 31(11): L11303

Science and Technology Committee of the People's Republic of China (STCPRC). 1964. Reports of Sino-Vietnamese Joint Comprehensive Marine Survey in the Beibu Gulf

Shi Maochong, Chen Changsheng, Xu Qichun, et al. 2002. The role of Qiongzhou Strait in the seasonal variation of the South China Sea circulation. Journal of Physical Oceanography, 32(1): 103–121

Su Jilan. 2005. Chinese Coastal Hydrology (in Chinese). Beijing: China Ocean Press

Sun Hongliang, Huang Weimin, Zhao Junsheng. 2001. Three-dimentional numerical simulation of tide-induced, wind-driven and thermohaline residual currents in the Beibu Bay. Oceanologia et

Limnologia Sinica (in Chinese), 32(5): 561–568

Sun Shuangwen, Wang Yi, Lan Jian. 2009. Hydrographic Condition and circulation in the Beibu Gulf in winter and summer of 2006. In: Li Yan, Hu Jianyu, eds. The Essay Collection of the Researches on the Ocean Science in the Gulf of Tonkin PT II (in Chinese). Beijing: China Ocean Press, 64–72

Trenberth K E, Large W G, Olson J G. 1990. The mean annual cycle in global ocean wind stress. Journal of Physical Oceanography, 20(11): 1742–1760

Wang Daoru. 1998. Study of the dynamic-thermodynamic mechanic of Beibu Bay cool water masses [dissertation] (in Chinese). Qingdao: Ocean University of China

Wu Dexing, Wang Yue, Lin Xiaopei, et al. 2008. On the mechanism of the cyclonic circulation in the Gulf of Tonkin in the summer. Journal of Geophysical Research: Oceans (1978–2012), 113(C9): doi: 10.1029/2007Jc004208

Xia Changshui, Qiao Fangli, Zhang Qinghua, et al. 2004. Numerical modelling of the quasi-global ocean circulation based on POM. Journal of Hydrodynamics, 16(5): 537–543

Xia Changshui, Qiao Fangli, Ma Jian, et al. 2006. Three-dimensional structure of the summertime circulation in the Yellow Sea from a wave-tide-circulation coupled model. Journal of Geophysical Research: Oceans (1978–2012), 111(C11): C11S03

Xia Huayong, Li Shuhua, Shi Maochong. 2001. A 3-D numerical simulation of wind-driven currents in the Beibu Gulf. Haiyang Xuebao (in Chinese), 23(6): 11–23

Xu Dongfeng, Yuan Yaochu, Liu Yuan. 2003. The baroclinic circulation structure of Yellow Sea cold water mass. Science in China Series D: Earth Sciences, 46(2): 117–126

Yang Yongzeng, Qiao Fangli, Zhao Wei, et al. 2005. MASNUM ocean wave numerical model in spherical coordinates and its application. Haiyang Xuebao (in Chinese), 27(2): 1–7

Zhao Baoren. 1985. The fronts of the Huanghai cold water mass (HCWM) induced by tidal mixing. Oceanologia et Limnologia Sinica (in Chinese), 16(6): 159–170

Zhao Chang, Lü Xingang, Qiao Fangli. 2010. Numerical study of the tidal waves in the Gulf of Tonkin. Haiyang Xuebao (in Chinese), 32(4): 1–11

Zhong Huanliang. 1995. Analysis of circulations in northern part of Beibu Gulf of South China Sea in spring. Marine Science Bulleten (in Chinese), 14(1): 81–84

Zu Tingting. 2005. Analysis of the current and its mechanism in the Gulf of Beibu [dissertation] (in Chinese). Qingdao: Ocean University of China

Zu Tingting, Gan Jianping, Erofeeva S Y. 2008. Numerical study of the tide and tidal dynamics in the South China Sea. Deep Sea Research: Part I. Oceanographic Research Papers, 55(2): 137–154